Table 2 Number of patients (%) by type of joint symptoms

	No. of patients
Joint symptoms	
Morning stiffness	44 (45.8%)
Arthralgia	44 (45.8%)
Myagia	6 (6.2%)
Others	2 (2%)
Total	96 (100%)

Table 3 Risk factors of anastrozole-related joint symptoms

No. of patients	Total	With joint symptoms	%	*P*
Age, years				
<65	227	77	33.9	0.0004
≥65	121	19	15.7	
BMI				
<23	199	61	30.6	0.137
≥23	149	35	23.4	
Adjuvant chemotherapy				
None	226	48	21.2	
Taxane or Epirubicin → Taxane	70	31	44.2	0.0004
Epirubicin	110	47	42.7	<0.0001
CMF	5	0	0	0.166

($P = 0.0004$) for those treated with taxane or sequential epirubicin and taxane therapy, and 42.7% ($P = 0.0004$) for those treated with epirubicin.

Bone fractures

Eight fractures occurred in the 348 patients with the fracture sites as shown in Table 4. Annual fracture rates were 0.86% (3/348) and 0.85% (2/234) during the first and second year, respectively, after the start of treatment with anastrozole (Fig. 1). Since the median follow-up period was 22 months and the number of patients treated with anastrozole for more than 2 years was so small, annual fracture rates are shown only for the first two years. These rates are lower than those reported for the Caucasian breast cancer patients in the ATAC trial (2.0 and 2.7%, respectively) (Buzdar et al. 2006).

Table 4 Bone fracture sites

	No. of patients
Bone fracture sites	
Shoulder	1
Clavicle	2
Wrist	2
Exfoliation	1
Spine	1
Jaw	1
Total	8

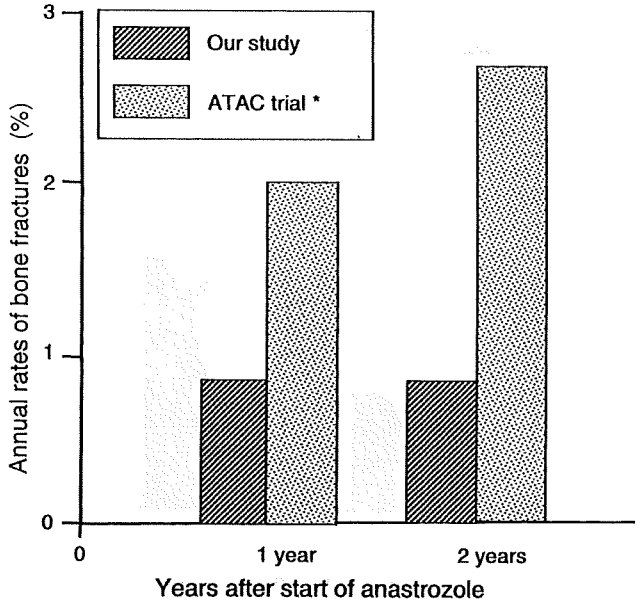

Fig. 1 Annual rates of bone fracture after start of anastrozole treatment (* Buzdar et al. 2006)

Infuluence of anastrozole on BMD

The 39 patients who showed normal BMD of the lumbar spine at baseline had their BMD measured serially 1 and 2 years after the start of anastrozole treatment (patients who were osteopenic or osteoporosis at baseline were excluded from this analysis). As shown in Fig. 2, lumbar BMD decreased by 1.3 and 2.8%, respectively. These reductions in lumbar BMD are smaller than those reported for the Caucasian breast cancer patients in the ATAC trial (2.2 and 4.0%, respectively) (Buzdar et al. 2006).

Discussion

According to the results of the ATAC trial, which compared the effects of adjuvant anastrozole and tamoxifen for Caucasian postmenopausal breast cancer patients, 35.6% of patients experienced joint symptoms, and the majority of the symptoms developed within 24 months after the start of treatment with a peak occurrence at 6 months. The median time to resolution of joint symptoms was reported as 5.5 months. Our study obtained essentially similar results for the incidence and clinical course of joint symptoms. Other studies have reported a similar incidence of

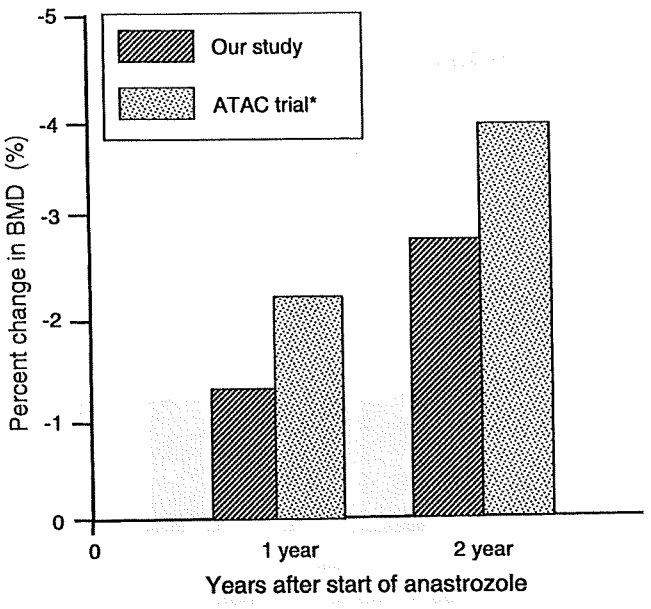

Fig. 2 Influence of anastrozole on BMD (* Buzdar et al. 2006)

anastrozole-related joint symptoms for Japanese women (Ohsako et al. 2006). It can therefore be concluded that the incidence of anastrozole-related joint symptoms and their clinical course are similar for Japanese and Caucasian postmenopausal breast cancer patients.

Although the exact mechanism of anastrozole-related joint symptoms is still unclear, Donnellan et al. suggest that a precipitous fall in estrogen levels is one cause of the observed joint symptoms (Donnellan et al. 2001). Andersen et al. also reported estrogen deficiency accelerates cartilage turnover and increases cartilage surface erosion (Andersen et al. 2004), suggesting that anastrozole-induced decrease in estrogen levels might play an important role in the pathogenesis of joint symptoms. Crew et al. reported that patients who have received prior taxane chemotherapy are more than four times more likely to develop anastrozole-related joint symptoms than those who have not (Crew et al. 2007). In the study presented here, we obtained similar results in that patients who received prior taxane or taxane-containing chemotherapy are at a higher risk for developing joint symptoms, and we also found that epirubicin-containing regimens can also be a significant risk factor for joint symptoms (Table 4).

Since BMD and bone fracture incidence are reported to be different for Japanese and Caucasian postmenopausal women in a general population (Ross et al. 1995) and since the hormonal milieu is also different, it was considered possible that the adverse effect of anastrozole on bone might also be different for these two ethnicities. The ATAC trial reports that annual rates of bone fractures are 2.0 and 2.7% for the first and second year, respectively, after the start of anastrozle treatment for Caucasian patients. In our study, however, we found that the corresponding rates for Japanese patients are 0.86 and 0.85% and thus appear to be lower than those reported for Caucasian women. Since the median follow-up period of our study is still short (22 months), the long-term adverse effect of anastrozole on bone fractures need to be investigated. Nevertheless, our results seem to indicate the possibility that there is an ethnic difference in bone fracture rates between Japanese and Caucasian patients.

We studied changes in BMD over time after the start of anastrozole treatment for patients with normal BMD and found that they lose 1.3 and 2.8% of BMD 1 and 2 years, respectively, after the start of the treatment. The subprotocol of the ATAC trial, on the other hand, shows that Caucasian women lose an average of 2.2 and 4.0% of BMD 1 and 2 years, respectively, after the start of anastrozole therapy. These results seem to suggest that Japanese women are likely to show a smaller reduction in BMD than Caucasian women do, which is compatible with our observation that Japanese patients have a lower incidence of bone fractures than Caucasian patients, although the difference in the patient population and in the method for BMD measurement used in these two studies makes a direct comparison inaccurate. It has been reported, however, that postmenopausal Caucasian women have higher serum estrogen levels and higher BMD than postmenopausal Japanese women (Shimizu et al. 1990; Ito et al. 1997). It is therefore reasonable to speculate that anastrozole treatment is likely to induce a more precipitous fall in estrogen levels in Caucasian patients than in Japanese patients, resulting in a greater reduction in BMD and a subsequent higher incidence of bone fractures in the former.

In conclusion, we have been able to show that the incidence of joint symptoms and their clinical course and risk factors is very similar for Japanese and Caucasian breast cancer patients treated with adjuvant anastrozole but that Japanese patients have a smaller reduction in BMD and a lower incidence of bone fractures than Caucasian patients after anastrozole treatment, probably due to ethnic differences in hormonal milieu. The possible ethnic difference in the adverse effect of anastrozole on bone considered in our study may be of considerable clinical importance and thus needs to be investigated in more detail and with a larger number of patients.

References

Andersen PH, Tanko LB, Andersen TL, Lundberg CV, Mo JA, Heegaard AM, Delaisse JM, Christgaus S (2004) Ovariectomized rats as a model of postmenopausal osteoarthritis: validation and application. Arthritis Res Ther 6:R169–R180

Baum M, Buzdar AU, Cuzick J, Forbes J, Houghton JH, Klijn JG, Sahmound T, ATAC Trialists' Group (2002) Anastrozole alone or

in combination with tamoxifen versus tamoxifen alone for adjuvant treatment of postmenopausal woman with early breast cancer: first results of the ATAC randomised trials. Lancet 359:2131–2139

Buzdar A, Howell A, Cuzick J, Wale C, Distler W, Hoctin-Boes G, Houghton J, Locker GY, Nabhholtz JM, ATAC Trialists' Group (2006) Comprehensive side-effect profile of anastrozole and tamoxifen as adjuvant treatment for early-stage breast cancer: long-term safety analysis of the ATAC trial. Lancet Oncol 7:633–643

Crew KD, Greenlee H, Capodice J, Raptis G, Brafman L, Fuentes D, Sierra A, Hershman DL (2007) Prevalence of joint symptoms in postmenopausal women taking aromotase inhibitors for early-stage breast cancer. J Clin Oncol 25:3877–3883

Donnellan PP, Douglas SL, Cameron DA, Leonard RC (2001) Aromatase inhibitors and arthralgia. J Clin Oncol 19:2767

Howell A, Cuzick J, Baum M, Buzdar A, Dowsett M, Forbes JF, Hoctin-Boes G, Houghton J, Locker GY, Tobias JS, ATAC Trialist's Group (2005) Results of the ATAC trial after completion of 5 years' adjuvant treatment for breast cancer. Lancet 365:60–62

Ito M, Lang TF, Jergas M, Ohki M, Takada M, Nakamura T, Hayashi K, Genanat HK (1997) Spinal trabecular bone loss and fracture in American and Japanese women. Calcif Tissue Int 61:123–128

Ohsako T, Inoue K, Nagamoto N, Yoshida Y, Nakahara O, Sakamoto N (2006) Joint symptoms: a practical problem of anastrozole. Breast Cancer 13:284–288

Ross PD, Fujiwara S, Huang C, Davis JW, Epstein RS, Wasnich RD, Kodama K, Melton LJ III (1995) Vertebral fracture prevalence in women in Hiroshima compared to Caucasians or Japanese in the US. Int J Epidemiol 24:1171–1177

Shimizu H, Ross RK, Bernstein L, Pike MC, Henderson BE (1990) Serum oestrogen levels in postmenopausal women: comparison of American whites and Japanese. Br J Cancer 62:451–453

Yoneda K, Tanji Y, Okishiro M, Taguchi T, Tamaki Y, Noguchi S (2006) Influence of adjuvant anastrozole on bone mineral density in Japanese postmenopausal breast cancer patients: is there a racial difference? Ann Oncol 17:1175–1176

Clinical Study

Oncology

Oncology 2009;77:134–139
DOI: 10.1159/000229753

Received: October 23, 2008
Accepted after revision: February 24, 2009
Published online: July 23, 2009

Good Response to Paclitaxel Predicts High Rates of Pathologic Complete Response for Breast Cancer Patients Treated Preoperatively with Paclitaxel Followed by 5-Fluorouracil, Epirubicin and Cyclophosphamide

Seung Jin Kim Tetsuya Taguchi Kenzo Shimazu Yoshio Tanji Yasuhiro Tamaki Shinzaburo Noguchi

Breast and Endocrine Surgery, Graduate School of Medicine, Osaka University, Osaka, Japan

Key Words
Breast cancer · Neoadjuvant chemotherapy · Predictor factor · Response

Abstract
Objective: Predictors of pathologic complete response (pCR) to neoadjuvant chemotherapy for breast cancers have been studied extensively. Here, we focused on reduction rate after paclitaxel administration for prediction of pCR to paclitaxel followed by 5-fluorouracil, epirubicin, and cyclophosphamide (FEC). ***Methods:*** This study included 115 patients with tumors ≥3.0 cm or with node-positive disease who were treated preoperatively with paclitaxel (80 mg/m^2, once a week, 12 cycles) followed by FEC (500/75/500 mg/m^2, every three weeks, 4 cycles). Reduction rate was measured with magnetic resonance imaging. ***Results:*** Tumor size (≤5.0 cm) ($p = 0.014$), estrogen receptor (ER) negativity ($p = 0.013$), and human epidermal growth factor receptor 2 positivity ($p = 0.020$), but not histologic type, histologic grade, or progesterone receptor, were significantly associated with pCR, while association of reduction rate ≥80% was highly significant ($p = 0.0003$). Multivariate analysis identified negative ER ($p = 0.022$) and reduction rate ($p = 0.003$) as independent predictors of pCR. Finally, patients with reduction rate ≥80% showed a significantly higher favorable outcome ($p = 0.014$) than others. ***Conclusions:*** Good response (reduction rate ≥80%) to paclitaxel seems to be a clinically useful predictor of pCR as well as a favorable prognosticator for patients treated preoperatively with paclitaxel followed by FEC.

Introduction

Neoadjuvant chemotherapy (NAC) has become the standard of care not only for inoperable but also for operable locally advanced breast cancer patients [1–3]. NAC offers the advantage that tumors can be downstaged, making previously inoperable tumors operable and enhancing the feasibility of breast-conserving surgery [4, 5]. In addition, several lines of evidence have demonstrated that patients who attain pathologic complete response (pCR) to NAC show a better prognosis than those without pCR, so that pCR is now considered to be the best prognosticator for patients treated with NAC [1–3, 6, 7]. Thus, many attempts have recently been made to develop clinically useful predictors of post-NAC pCR, including a variety of clinicopathologic parameters such as histo-

KARGER
Fax +41 61 306 12 34
E-Mail karger@karger.ch
www.karger.com

0030–2414/09/0772–0134$26.00/0

Accessible online at:
www.karger.com/ocl

Shinzaburo Noguchi, MD, PhD
Breast and Endocrine Surgery
Graduate School of Medicine, Osaka University
2-2-E-10 Yamadaoka, Suita City, Osaka 565-0871 (Japan)
Tel. +81 6 6879 3772, Fax +81 6 6879 3779, E-Mail noguchi@onsurg.med.osaka-u.ac.jp

logic grade, estrogen receptor (ER), progesterone receptor (PR) status, human epidermal growth factor receptor 2 (HER2) as well as gene-expression profiling [8–11]. These parameters have been evaluated for their ability to predict pCR and some associations of these parameters with pCR have been reported, but their clinical value remains unconvincing so that a more precise predictor of pCR needs to be developed.

Sequential chemotherapy consisting of paclitaxel and an anthracycline-based regimen (5-fluorouracil, epirubicin or doxorubicin, and cyclophosphamide), known as FEC or FAC, is now widely accepted as a highly efficacious NAC [2, 3, 7, 8, 12, 13]. Our study focused on response to initial paclitaxel therapy as a predictor of pCR after administration of sequential paclitaxel and FEC. Since tumors which respond well to initial chemotherapy are generally more likely to show a more favorable response to subsequent chemotherapy than initial nonresponders, we hypothesized that responsiveness to initial chemotherapy would be a good predictor of response to second-line chemotherapy.

The aim of this study was therefore to examine the association between response to initial paclitaxel therapy and pCR after completion of paclitaxel followed by FEC and to compare its value as a pCR predictor with that of other conventional predictors. Since we considered a highly accurate evaluation of the response to initial paclitaxel therapy as essential, we monitored tumor size before and after paclitaxel with magnetic resonance imaging (MRI), which is considered to be the most accurate modality for assessment of tumor size after NAC [14–16].

Patients and Methods

Patients

Primary breast cancer patients with tumors ≥3.0 cm in diameter or with cytologically confirmed lymph node involvement, but excluding those with stage IV diseases, were recruited for this study. All patients underwent a vacuum-assisted core needle biopsy to confirm the presence of invasive breast cancer before NAC. After informed consent was obtained, patients were treated with paclitaxel (80 mg/m^2, weekly for 12 cycles) followed by FEC (500/75/500 mg/m^2, every three weeks, 4 cycles) [13]. After NAC, patients were treated with breast-conserving surgery followed by radiation therapy or mastectomy (radiation therapy for the chest wall was added for more than 3 positive lymph nodes).

All patients with hormone-receptor-positive (ER and/or PR positive) tumors were given adjuvant hormone therapy (tamoxifen plus goserelin for premenopausal, and tamoxifen or anastrozole for postmenopausal patients) essentially according to the guidelines of the St. Gallen consensus meeting [17]. No patients received chemotherapy after surgery. Of the 115 patients, 110 patients completed NAC as scheduled, but 2 patients received 11 cycles of paclitaxel and 3 patients received 3 cycles of FEC. Dose was not reduced in any patients. No patient developed cardiac adverse events. Of 32 patients with HER2-positive tumors, no patients were treated with trastuzumab preoperatively, but 11 pa-

Table 1. Patient characteristics (n = 115)

Category	
Age, years	
Range	23–72
Mean	49.5
Menopausal status	
Premenopausal	58 (50%)
Postmenopausal	57 (50%)
Clinical stage	
IIA	26 (23%)
IIB	45 (39%)
IIIA	28 (24%)
IIIB	14 (12%)
IIIC	2 (2%)
Tumor size	
≤5.0 cm	78 (68%)
>5.0 cm	37 (32%)
Histology	
Invasive ductal cancer	105 (91%)
Invasive lobular cancer	8 (7%)
Others	2 (2%)
Histologic grade[1]	
I	13 (11%)
II	77 (68%)
III	24 (21%)
ER	
Positive	70 (61%)
Negative	45 (39%)
PR	
Positive	40 (35%)
Negative	75 (65%)
HER2[2]	
Negative	82 (72%)
Positive	32 (28%)
Surgery	
Mastectomy	86 (75%)
Breast-conserving surgery	29 (25%)
Adjuvant endocrine therapy	
No	37 (32%)
Tamoxifen	14 (12%)
Tamoxifen + LHRH analog	20 (17%)
Aromatase inhibitors	44 (38%)
Adjuvant trastuzumab	
Yes	11 (10%)
No	104 (90%)

[1] One sample was not available.
[2] One sample was not evaluated.

Table 2. Association between clinicopathologic parameters and pCR

Parameters	Category	pCR		p value[1]
		yes (n = 29)	no (n = 86)	
Menopausal status	pre-	11 (19%)	47 (81%)	0.119
	post-	18 (32%)	39 (68%)	
Tumor size, cm	≤5.0	25 (32%)	53 (68%)	0.014
	>5.0	4 (11%)	33 (89%)	
Histologic type	IDC	28 (27%)	77 (73%)	0.177
	ILC	0 (0%)	8 (100%)	
	mucinous	1 (50%)	1 (50%)	
Histologic grade[2]	1	4 (31%)	9 (69%)	0.847
	2	18 (23%)	59 (77%)	
	3	6 (25%)	18 (75%)	
ER	positive	12 (17%)	58 (83%)	0.013
	negative	17 (38%)	28 (62%)	
PR	positive	7 (18%)	33 (83%)	0.164
	negative	22 (29%)	53 (71%)	
HER2[2]	negative	16 (20%)	66 (80%)	0.020
	positive	13 (41%)	19 (59%)	
ER/HER2	(+)/(−)	8 (15%)	46 (85%)	0.010
	(+)/(+)	4 (25%)	12 (75%)	
	(−)/(−)	8 (29%)	20 (71%)	
	(−)/(+)	9 (56%)	7 (44%)	
WHO criteria	non-responders	2 (9%)	21 (91%)	0.041
	responders	27 (29%)	65 (71%)	
RECIST	non-responders	4 (13%)	26 (87%)	0.081
	responders	25 (29%)	60 (71%)	
Reduction rate after paclitaxel	<80%	7 (11%)	54 (89%)	0.0003
	≥80%	22 (41%)	32 (59%)	

IDC = invasive ductal carcinoma; ILC = invasive lobular carcinoma.

[1] p value was evaluated with the χ^2 test, and considered significant when $p < 0.05$.

[2] One sample was not evaluated.

tients received trastuzumab postoperatively. Median follow-up after surgery was 20 months, ranging from 6 to 53 months. Patient characteristics are summarized in table 1.

Hormone Receptor and HER2 Assay

ER and PR were determined by immunohistochemistry (IHC) with a cut-off value of 10%. HER2 expression was examined with IHC (Herceptest®; Dako Corporation, Carpenteria, Calif., USA) or fluorescence in situ hybridization (FISH) (Pathvysion®; Vysis Inc., Downers Grove, Ill., USA). Tumors with IHC (3+) or FISH (+) were considered HER2 positive.

Evaluation of Clinical and Pathologic Response to Chemotherapy

Clinical response of primary breast tumors to paclitaxel was evaluated with dynamic MRI before and after paclitaxel administration. Response to paclitaxel was evaluated with ultrasonography in 17 patients who did not undergo dynamic MRI. Reduction rate was calculated with the following formula: reduction rate (%) = (tumor area before paclitaxel − tumor area after paclitaxel)/tumor area before paclitaxel × 100. Pathologic response was evaluated in specimens obtained at surgery. pCR was defined as absence of residual invasive foci and no lymph node involvement.

Statistical Methods

Associations of clinicopathologic parameters with pCR were evaluated with the χ^2 test. Multivariate analysis of the relationship of negative ER and reduction rate (≥80%) with pCR was determined using a logistic regression method to obtain the odds ratio and 95% confidence interval. Relapse-free survival (RFS) rates were estimated with the Kaplan-Meier method, and differences were evaluated with the log-rank test. All test results with a p value of less than 0.05 were considered significant. All statistical analyses were performed with StatView™ software (SAS Institute Inc., Cary, N.C., USA).

Results

Association of Clinicopathologic Parameters with pCR

The association of clinicopathologic parameters with pCR was analyzed in 115 patients, and pCR was observed in 29 (25%) of them. Table 2 shows associations between pCR and various clinicopathologic parameters. Menopausal status, histologic type, histologic grade, and PR status were not significantly associated with pCR, although it was noteworthy that none of the 8 invasive lobular carcinomas attained pCR. Tumors ≤5.0 cm (pCR rate: 32%), ER-negative tumors (38%), and HER2-positive tumors (41%) were significantly more likely to attain pCR than tumors >5.0 cm (11%, p = 0.014), ER-positive tumors (17%, p = 0.013), and HER2-negative tumors (20%, p = 0.020). Analysis of ER and HER2 combined showed that ER-negative and HER2-positive tumors were most likely (56%), and ER-positive and HER2-negative tumors most unlikely to attain pCR (15%). ER-positive and HER2-positive tumors (25%) and ER-negative and HER2-negative tumors (29%) showed intermediate pCR rates.

Association of Reduction Rate after Paclitaxel with pCR

There was a significant association between MRI-evaluated reduction rates after paclitaxel and pCR rates (fig. 1). Tumors with a reduction rate ≥50%, equivalent to complete response and partial response by WHO criteria, were likely to attain pCR compared with those with

a reduction rate <50% (pCR rate, 29 vs. 9%, p = 0.041), and those with a reduction rate ≥80% were significantly more likely to attain pCR than those with a reduction rate <80% (pCR rate, 41 vs. 11%, p = 0.0003) (fig. 2, 3, table 2). Responders (complete response + partial response) classified by Response Evaluation Criteria In Solid Tumors (RECIST) had a tendency to attain pCR compared with nonresponders, but the difference was not statistically significant (pCR rate, 29 vs. 13%, p = 0.081) (table 2).

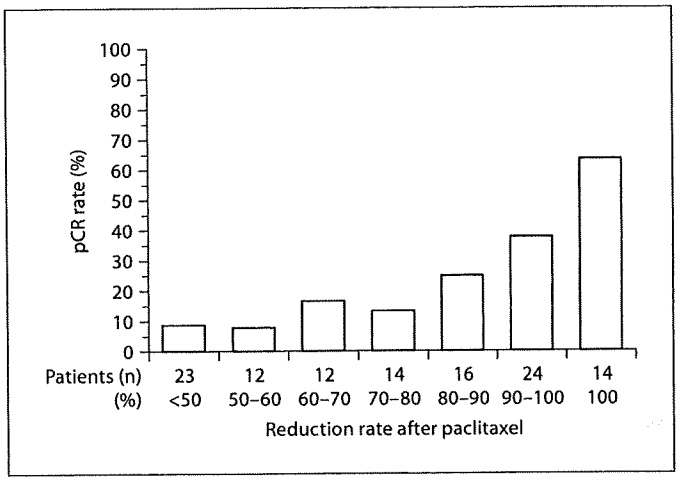

Fig. 1. pCR rates for paclitaxel followed by FEC in relation to reduction rate after paclitaxel. pCR rates were 64% for a reduction rate of 100%, 38% for a 100% > reduction rate ≥ 90%, 25% for a 90% > reduction rate ≥ 80%, 14% for an 80% > reduction rate ≥ 70%, 17% for a 70% > reduction rate ≥ 60%, 8% for a 60% > reduction rate ≥ 50%, and 9% for a 50% > reduction rate.

Univariate and Multivariate Analysis of Predictors for pCR

Univariate analysis demonstrated that small tumor size (p = 0.020), ER negativity (p = 0.015), HER2 positivity (p = 0.023), and a reduction rate ≥80% after paclitaxel (p = 0.001) are significantly associated with pCR. Multivariate analysis showed that ER (p = 0.022) and reduction rate (p = 0.003) are significant and independent predictors of pCR (table 3).

Association of pCR or Reduction Rate after Paclitaxel with Prognosis

None of the 29 patients who attained pCR developed recurrences, whereas 14 of the 86 patients who could not attain pCR did (p = 0.026). Patients with a reduction rate ≥80% after paclitaxel showed significantly better RFS rates than those with a reduction rate <80% (events, $^{2}/_{54}$ vs. $^{12}/_{61}$, p = 0.014).

Discussion

Many studies have focused on the development of predictors of pCR for NAC. Several investigators have demonstrated that ER-negative or HER2-positive tumors are

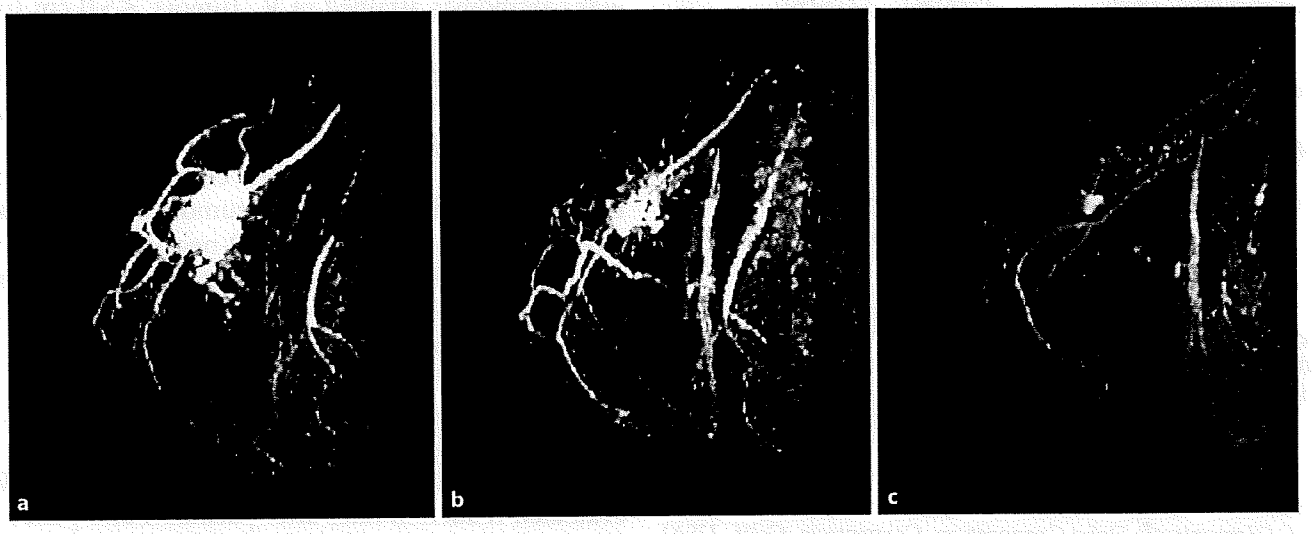

Fig. 2. Contrast-enhanced MRI images in a 72-year-old woman with <80% of tumor shrinkage after paclitaxel. **a** Before paclitaxel. **b** Reduction rate was 66% after paclitaxel. **c** The final reduction rate was 93% after the completion of paclitaxel followed by FEC. Her tumor did not attain pCR.

significantly associated with pCR [7–10]. In addition, recent review works have shown that not only anthracycline-based regimens but also taxane-containing regimens provide more benefit in patients with HER2-positive tumors than in those with HER2-negative tumors [18, 19]. Our results also showed that ER-negative and HER2-positive tumors are significantly more likely than ER-positive and HER2-negative tumors to attain pCR to paclitaxel followed by FEC (pCR rate, 56 vs. 15%), indicating that ER and HER2 can serve as significant predictors of pCR to paclitaxel followed by FEC. However, the percentage of patients with ER-negative and HER2-positive disease is small (14%) in all patients.

Besides ER and HER2, we focused on response to paclitaxel as a novel predictor of pCR to paclitaxel followed by FEC because tumors with pCR after the completion of this neoadjuvant regimen often show a good response to initial paclitaxel. Using common criteria, i.e., WHO or RECIST, as many as approximately 80% of patients were classified as responders (complete response + partial response) to paclitaxel and such clinical responses did not show a strong correlation with pCR (table 2). Therefore, we employed a stricter cut-off value (reduction rate ≥80%). pCR was observed in 22 (41%) of the 54 tumors with a reduction rate ≥80% in response to paclitaxel and in 7 (11%) of the 61 with a reduction rate <80%. These results indicate that a good response to paclitaxel can serve as a significant predictor of pCR. Multivariate analysis demonstrated that response to paclitaxel is a significant predictor of pCR, which is independent of ER and HER2. In addition, we were able to show that response to paclitaxel also serves as a prognostic indicator, i.e., patients with a good response show a significantly better prognosis than those with a poor response. However, our present data should be interpreted with great caution due to the following reasons. Firstly, 41% of patients with tumors with pCR had ER-positive disease and

Table 3. Uni- and multivariate analyses of pCR

	Univariate			Multivariate		
	OR	95% CI	p	OR	95% CI	p
Tumor size						
≤5.0 cm vs. >5.0 cm	3.9	1.2–12.2	0.020	3.0	0.9–10.2	0.076
ER						
(–) vs. (+)	2.9	1.2–7.0	0.015	3.2	1.2–8.7	0.022
HER2						
(+) vs. (–)	2.8	1.2–6.9	0.023	1.9	0.7–5.4	0.226
Reduction rate after paclitaxel						
≥80% vs. <80%	5.3	2.0–13.8	0.001	4.9	1.7–14.1	0.003

p value was considered significant when $p < 0.05$. OR = Odds ratio; CI = confidence interval.

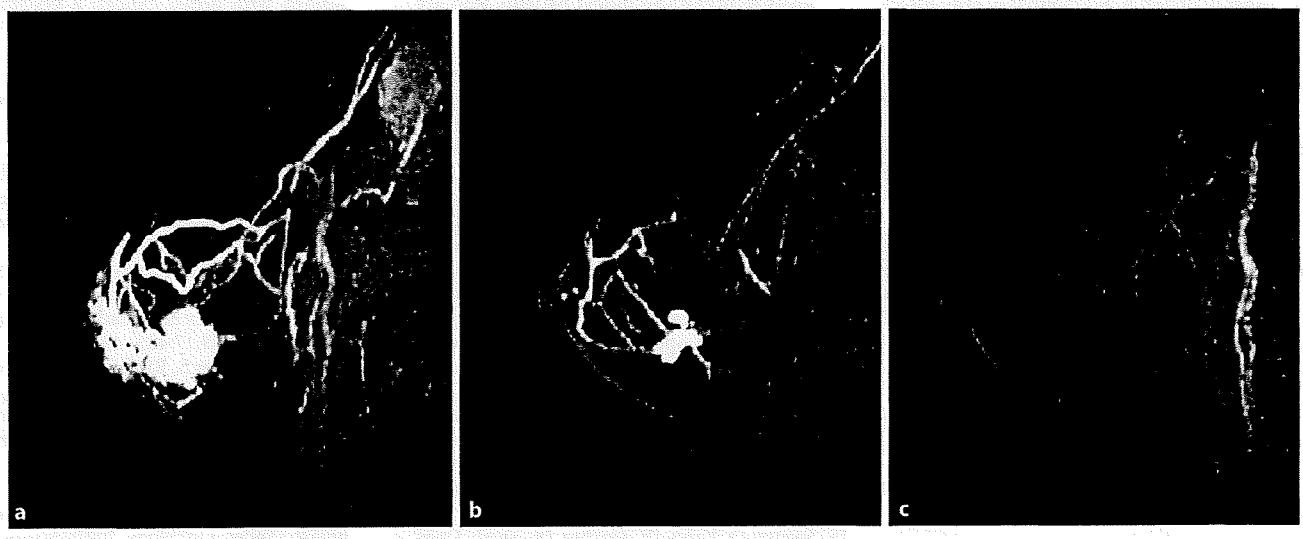

Fig. 3. Contrast-enhanced MRI images in a 60-year-old woman with ≥80% of tumor shrinkage after paclitaxel. **a** Before paclitaxel. **b** Reduction rate was 80% after paclitaxel. **c** The final reduction rate was 100% after the completion of paclitaxel followed by FEC. Her tumor attained pCR.

were treated with adjuvant endocrine therapy. Secondly, the present study is a retrospective study at a single institute, and lastly, this study has a very short follow-up period.

Our observations seem to be consistent with the results of the Aberdeen neoadjuvant trial [20], where patients who showed a good response to the initial anthracycline-based chemotherapy and switched to subsequent docetaxel attained a high pCR rate (34%) while those who showed a poor initial response and switched to docetaxel attained a low pCR rate (2%). Our results together with those of the Aberdeen neoadjuvant trial suggest that breast tumors responsive to taxane- and those responsive to anthracycline-based chemotherapy show considerable overlap, and such overlapping tumors can be expected to show a rather good response to sequential taxane- and anthracycline-based chemotherapy, with pCR as the result. Thus, patients who show a good response to paclitaxel are definite candidates for subsequent FEC since they have a very good chance to attain pCR, but those who show a poor response to paclitaxel can be expected to attain a very low pCR rate as well as a poor prognosis. For the latter group, administration of other chemotherapies proven to be effective for tumors resistant to paclitaxel- and anthracycline-based chemotherapy, i.e., capecitabine, vinorelbine, or gemicitabine, should be considered [21–23].

In conclusion, we were able to show that, in addition to ER and HER2, response to paclitaxel can serve as a significant predictor of pCR for patients preoperatively treated with paclitaxel followed by FEC. Prediction of pCR based on response to initial paclitaxel might be useful for choosing the second-line chemotherapy and might serve as a surrogate marker of prognosis, although our findings need to be validated by a future study including a larger number of patients.

References

1 Kaufmann M, Hortobagyi GN, Goldhirsch A, et al: Recommendations from an international expert panel on the use of neoadjuvant (primary) systemic treatment of operable breast cancer: an update. J Clin Oncol 2006; 24:1940–1949.
2 Buzdar AU: Preoperative chemotherapy treatment of breast cancer – a review. Cancer 2007;110:2394–2407.
3 Charfare H, Limongelli S, Purushotham AD: Neoadjuvant chemotherapy in breast cancer. Br J Cancer 2005;92:14–23.
4 Fisher B, Brown A, Mamounas E, et al: Effect of preoperative chemotherapy on loco-regional disease in women with operable breast cancer: findings from National Surgical Adjuvant Breast and Bowel Project B-18. J Clin Oncol 1997;15:2483–2493.
5 Makris A, Powles TJ, Ashley SE, et al: A reduction in the requirements for mastectomy in a randomized trial of neoadjuvant chemoendocrine therapy in primary breast cancer. Ann Oncol 1998;9:1179–1184.
6 Kuerer HM, Newman LA, Smith TL, et al: Clinical course of breast cancer patients with complete pathologic primary tumor and axillary lymph node response to doxorubicin-based neoadjuvant chemotherapy. J Clin Oncol 1999;17:460–469.
7 Rastogi P, Anderson SJ, Bear HD, et al: Preoperative chemotherapy: updates of National Surgical Adjuvant Breast and Bowel Project Protocols B-18 and B-27. J Clin Oncol 2008;26:778–785.
8 Mazouni C, Kau SW, Frye D, et al: Inclusion of taxanes, particularly weekly paclitaxel, in preoperative chemotherapy improves pathologic complete response rate in estrogen receptor-positive breast cancers. Ann Oncol 2007;18:874–880.
9 Colleoni M, Viale G, Zahrieh D, et al: Expression of ER, PgR, HER1, HER2, and response: a study of preoperative chemotherapy. Ann Oncol 2008;19:465–472.
10 Goldstein NS, Decker D, Severson D, et al: Molecular classification system identifies invasive breast carcinoma patients who are most likely and those who are least likely to achieve a complete pathologic response after neoadjuvant chemotherapy. Cancer 2007; 110:1687–1696.
11 Iwao-Koizumi K, Matoba R, Ueno N, et al: Prediction of docetaxel response in human breast cancer by gene expression profiling. J Clin Oncol 2005;23:422–431.
12 Cuppone F, Bria E, Carlini P, et al: Taxanes as primary chemotherapy for early breast cancer. Cancer 2008;113:238–246.
13 Green MC, Buzdar AU, Smith T, et al: Weekly paclitaxel improves pathologic complete remission in operable breast cancer when compared with paclitaxel once every 3 weeks. J Clin Oncol 2005;23:5983–5992.
14 Padhani AR, Hayes C, Assersohn L, et al: Prediction of clinicopathologic response of breast cancer to primary chemotherapy at contrast-enhanced MR imaging. Radiology 2006;239:361–374.
15 Segara D, Krop IE, Garber JE, et al: Does MRI predict pathologic tumor response in women with breast cancer undergoing preoperative chemotherapy? J Surg Oncol 2007; 96:474–480.
16 Chen JH, Feig B, Agrawal G, et al: MRI evaluation of pathologically complete response and residual tumors in breast cancer after neoadjuvant chemotherapy. Cancer 2008; 112:17–26.
17 Goldhirsch A, Glick JH, Gelber RD, et al: Meeting highlights: international expert consensus on the primary therapy of early breast cancer 2005. Ann Oncol 2005;16: 1569–1583.
18 Dhesy-Thind B, Pritchard KI, Messersmith H, et al: HER2/neu in systemic therapy for women with breast cancer: a systemic review. Breast Cancer Res Treat 2008;109:209–229.
19 Pritchard KI, Messersmith H, Elavathil L, et al: HER-2 and Topoisomerase II as predictors of response to chemotherapy. J Clin Oncol 2008;26:736–744.
20 Smith IC, Heys SD, Hutcheon AW, et al: Neoadjuvant chemotherapy in breast cancer: significantly enhanced response with docetaxel. J Clin Oncol 2002;20:1456–1466.
21 Blum JL, Jones SE, Buzdar AU, et al: Multicenter phase II study of capecitabine in paclitaxel-refractory metastatic breast cancer. J Clin Oncol 1999;17:485–493.
22 Zelek L, Barthier S, Riofrio M, et al: Weekly vinorelbine is an effective palliative regimen after failure with anthracyclines and taxanes in metastatic breast carcinoma. Cancer 2001; 92:2267–2272.
23 Seidman AD: Gemcitabine as single-agent therapy in the management of advanced breast cancer. Oncology 2001;15(suppl):11–14.

Published Online First on September 8, 2009 as 10.1158/0008-5472.CAN-09-1289

Priority Report

mTOR Signal and Hypoxia-Inducible Factor-1α Regulate CD133 Expression in Cancer Cells

Kazuko Matsumoto,[1] Tokuzo Arao,[1] Kaoru Tanaka,[1] Hiroyasu Kaneda,[1] Kanae Kudo,[1] Yoshihiko Fujita,[1] Daisuke Tamura,[1] Keiichi Aomatsu,[1] Tomohide Tamura,[3] Yasuhide Yamada,[3] Nagahiro Saijo,[2] and Kazuto Nishio[1]

[1]Department of Genome Biology, [2]Kinki University School of Medicine, Osaka-Sayama, Osaka, Japan; and [3]Department of Medical Oncology, National Cancer Center Hospital, Chuo-ku, Tokyo, Japan

Abstract

The underlying mechanism regulating the expression of the cancer stem cell/tumor-initiating cell marker CD133/prominin-1 in cancer cells remains largely unclear, although knowledge of this mechanism would likely provide important biological information regarding cancer stem cells. Here, we found that the inhibition of mTOR signaling up-regulated CD133 expression at both the mRNA and protein levels in a CD133-overexpressing cancer cell line. This effect was canceled by a rapamycin-competitor, tacrolimus, and was not modified by conventional cytotoxic drugs. We hypothesized that hypoxia-inducible factor-1α (HIF-1α), a downstream molecule in the mTOR signaling pathway, might regulate CD133 expression; we therefore investigated the relation between CD133 and HIF-1α. Hypoxic conditions up-regulated HIF-1α expression and inversely down-regulated CD133 expression at both the mRNA and protein levels. Similarly, the HIF-1α activator deferoxamine mesylate dose-dependently down-regulated CD133 expression, consistent with the effects of hypoxic conditions. Finally, the correlations between CD133 and the expressions of HIF-1α and HIF-1β were examined using clinical gastric cancer samples. A strong inverse correlation ($r = -0.68$) was observed between CD133 and HIF-1α, but not between CD133 and HIF-1β. In conclusion, these results indicate that HIF-1α down-regulates CD133 expression and suggest that mTOR signaling is involved in the expression of CD133 in cancer cells. Our findings provide a novel insight into the regulatory mechanisms of CD133 expression via mTOR signaling and HIF-1α in cancer cells and might lead to insights into the involvement of the mTOR signal and oxygen-sensitive intracellular pathways in the maintenance of stemness in cancer stem cells. [Cancer Res 2009;69(18):7160–4]

Introduction

The CD133/prominin-1 protein is a five-transmembrane molecule expressed on the cell surface that is widely regarded as a stem cell marker. Growing evidence indicates that CD133 can be used as a cell marker for cancer stem cells or tumor-initiating cells in colon cancer, prostate cancer, pancreatic cancer, hepatocellular carcinoma, neural tumors, and renal cancer (1). Strict regulatory mechanisms governing CD133 expression are thought to be deeply related to inherent cancer stemness; however, such mechanisms remain largely unclear, especially in cancer cells. In brain tumors, the Hedgehog (2), bone morphogenetic protein (3), and Notch (4) signaling pathways have been implicated in the control of CD133+ cancer stem cell function.

Some investigators have shown a relation between hypoxia and CD133 expression in brain tissue. The percentage of CD133-expressing cells was found to increase in a glioma cell line cultured under hypoxic conditions (5), and mouse fetal cortical precursors cultured under normoxic conditions exhibited a reduction in CD133(hi)CD24(lo) multipotent precursors and the failure of the remaining CD133(hi)CD24(lo) cells to generate glia (6). With the exception of these studies in brain tissue, however, data on the expression of CD133 and the involvement of hypoxia and other signaling pathways in cancer cells remains limited.

Several reports have indicated that mTOR is a positive regulator of hypoxia-inducible factor (HIF) expression and activity (7), and the inhibition of HIF-mediated gene expression is considered to be related to the antitumor activity of mTOR inhibitors in renal cell carcinoma (8). We found that mTOR signaling was involved in CD133 expression in gastric and colorectal cancer cells. Thus, we investigated the regulatory mechanism of CD133 in cancer cells.

Materials and Methods

Reagents. 5-Fluorouracil, irinotecan (CPT-11), and rapamycin were purchased from Sigma-Aldrich. Gemcitabine was provided by Eli Lilly. Tacrolimus (LKT Laboratories), LY294002 and wortmannin (Cell Signaling Technology), and deferoxamine mesylate (DFO; Sigma-Aldrich) were purchased from the indicated companies.

Cell cultures and hypoxic conditions. All of the 28 cell lines used in this study were maintained in RPMI 1640 (Sigma) supplemented with 10% heat-inactivated fetal bovine serum (Life Technologies), except for LoVo (F12; Nissui Pharmaceutical), WiDr, IM95, and HEK293 (DMEM; Nissui Pharmaceutical), and Huvec (Humedia; Kurabo). Hypoxic conditions (0.1% O_2) were achieved using the AnaeroPouch-Anaero (Mitsubishi Gas Chemical) with monitoring using an oxygen indicator.

Real-time reverse transcription-PCR. The methods were previously described (9). The primers used for the real-time reverse transcription-PCR (RT-PCR) were as follows: CD133, forward 5′-AGT GGC ATC GTG CAA ACC TG-3′ and reverse 5′-CTC CGA ATC CAT TCG ACG ATA GTA-3′; glyceraldehyde-3-phosphate dehydrogenase (GAPD), forward 5′-GCA CCG TCA AGG CTG AGA AC-3′ and reverse 5′-ATG GTG GTG AAG ACG CCA GT-3′. GAPD was used to normalize the expression levels in the subsequent quantitative analyses.

Clinical samples. The mRNA expression levels of CD133, HIF-1α, and HIF-1β in gastric cancer specimens were obtained from previously published microarray data (9).

Note: Supplementary data for this article are available at Cancer Research Online (http://cancerres.aacrjournals.org/).

K. Matsumoto and T. Arao contributed equally to this work.

Requests for reprints: Kazuto Nishio, Department of Genome Biology, Kinki University School of Medicine, 377-2 Ohno-higashi, Osaka-Sayama, Osaka 589-8511, Japan. Phone: 81-72-366-0221; Fax: 81-72-366-0206; E-mail: knishio@med.kindai.ac.jp.

doi:10.1158/0008-5472.CAN-09-1289

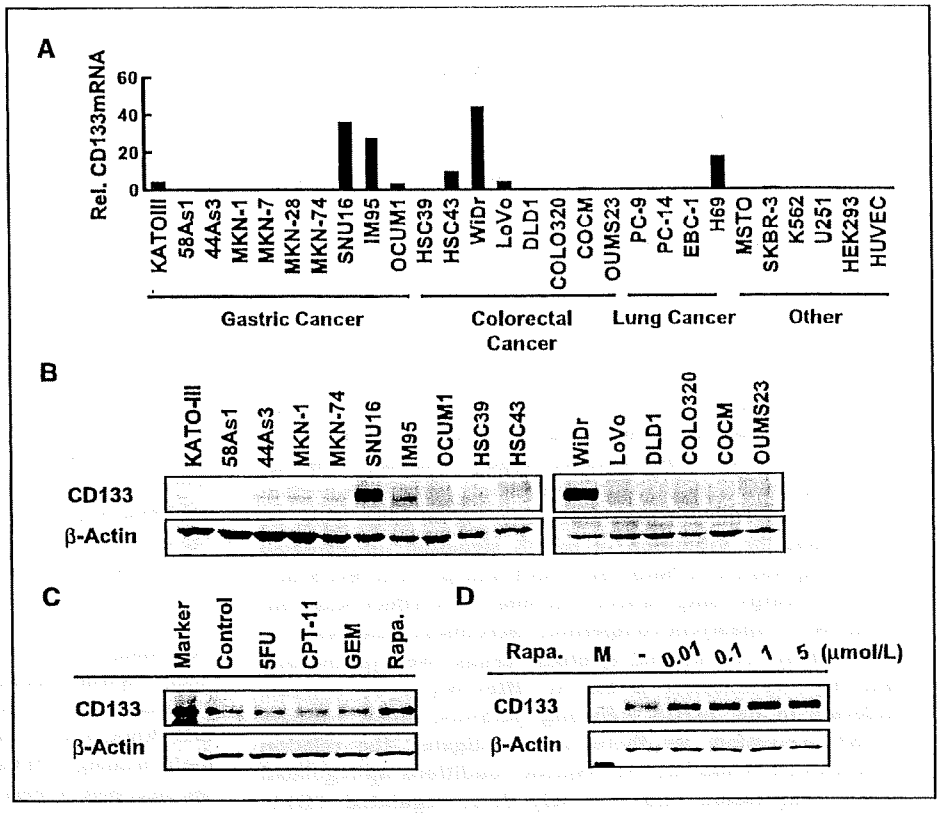

Figure 1. Rapamycin up-regulates CD133 expression. *A*, the mRNA expression levels of CD133 were examined using real-time RT-PCR in 26 cancer cell lines. *B*, the protein expressions of CD133 were determined using Western blotting in 16 gastric and colorectal cancer cell lines. *C*, Western blot of CD133 expression in WiDr cells exposed to cytotoxic drugs [1 μmol/L of 5-fluorouracil (*5-FU*), CPT-11, and gemcitabine (*GEM*)] and rapamycin (1 μmol/L) for 48 h. Note that only rapamycin up-regulates CD133 expression. *D*, WiDr cells were exposed to rapamycin at the indicated concentrations (0, 0.01, 0.1, 1, and 5 μmol/L) for 48 h. Rapamycin dose-dependently up-regulated CD133 expression. *Rel. CD133 mRNA*, normalized mRNA expression levels (CD133/GAPD × 10^4); *Rapa.*, rapamycin.

Immunoblotting. A Western blot analysis was performed as described previously (10). The experiment was performed in triplicate. The following antibodies were used: monoclonal CD133 antibody (W6B3C1; Miltenyi Biotec), rabbit polyclonal HIF-1α antibody (Novus Biologicals, Inc.), β-actin antibody, and HRP-conjugated secondary antibody (Cell Signaling Technology).

Results

Inhibition of the mTOR signal up-regulates CD133 expression in CD133-overexpressing gastrointestinal cancer cells. We examined the mRNA expression levels of CD133 in 26 cancer cell

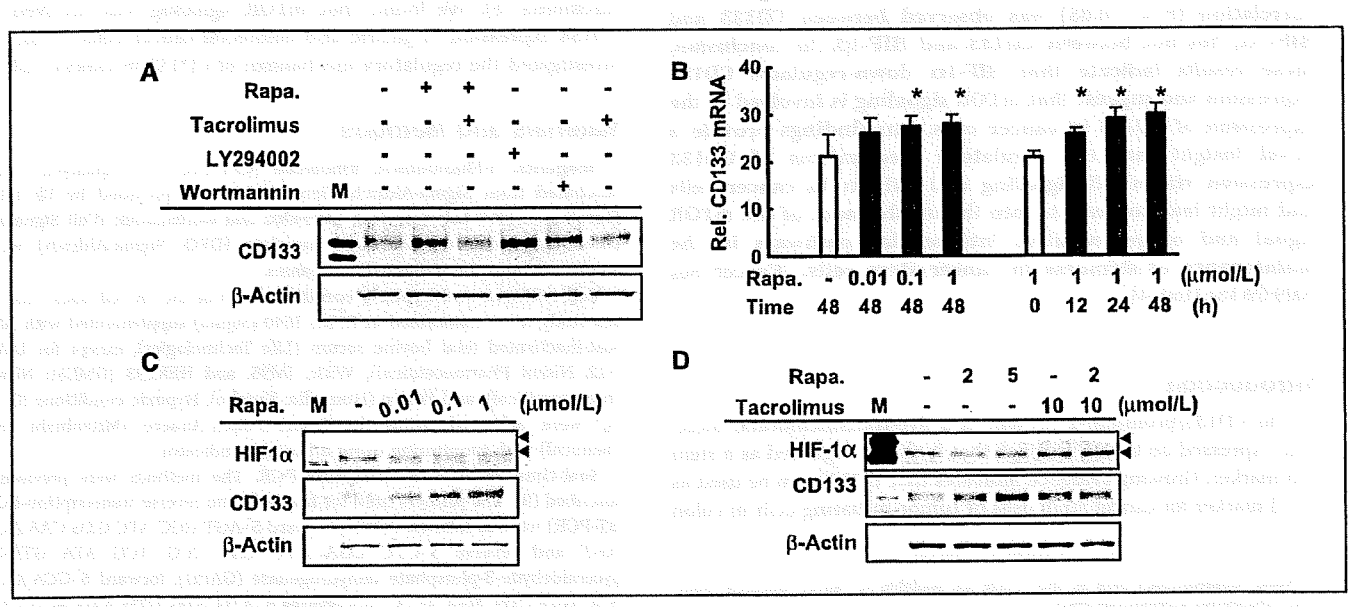

Figure 2. Rapamycin down-regulates HIF-1α expression and up-regulates CD133 expression at the transcriptional level. *A*, WiDr cells were exposed to rapamycin, the rapamycin-competitor tacrolimus, and the phosphoinositide-3-kinase inhibitors LY294002 and wortmannin for 48 h at concentrations of 10 μmol/L. The inhibition of mTOR signaling up-regulated CD133 expression. *B*, rapamycin up-regulated the expression of CD133 mRNA in WiDr cells in a time-dependent and dose-dependent manner. *Columns*, mean determined using real-time RT-PCR; *bars*, SD. *C* and *D*, rapamycin exposure and HIF-1α expression. WiDr cells were exposed to rapamycin with/without tacrolimus at the indicated concentration for 48 h. Rapamycin down-regulated HIF-1α expression and inversely up-regulated CD133 expression; these effects were canceled by tacrolimus. *Rel. CD133 mRNA*, normalized mRNA expression levels (CD133/GAPD × 10^4); *Rapa.*, rapamycin.

lines using real-time RT-PCR. Several gastric, colorectal, and lung cancer cell lines such as SNU16, IM95, HSC43, WiDr, and H69, overexpressed CD133 (Fig. 1*A*). The increased expression of CD133 protein was also confirmed in these cell lines (Fig. 1*B*). The mTOR inhibitor rapamycin, but not cytotoxic drugs (5-fluorouracil, CPT-11, and gemcitabine), increased the expression of CD133 in a dose-dependent manner in CD133-overexpressing WiDr cells (Fig. 1*C* and *D*). These results indicate that mTOR signaling is involved in the expression of CD133 in cancer cells.

Rapamycin down-regulated HIF-1α expression and up-regulated CD133 expression at the transcriptional level. To examine the signal transduction of rapamycin-induced CD133 expression, we used the rapamycin-competitor tacrolimus and the phosphoinositide-3-kinase inhibitors LY294002 and wortmannin. Tacrolimus (10 μmol/L) completely canceled the up-regulation of CD133 induced by rapamycin. The inhibition of phosphoinositide-3-kinase by LY294002 (10 μmol/L) and wortmannin (10 μmol/L) also up-regulated CD133 expression (Fig. 2*A*). Rapamycin up-regulated CD133 expression at the transcriptional level in a dose-dependent and time-dependent manner (Fig. 2*B*).

The inhibition of mTOR signaling is likely to lead to the down-regulation of the expression of certain molecules because the mTOR complex positively regulates the general translational machinery. Under the inhibition of mTOR signaling, HIF-1α, among several downstream molecules of mTOR, can activate transcription by acting as a repressor of specific transcription factors such as the MYC-associated protein X homodimer (11). Therefore, we focused on the possible role of HIF-1α in the regulation of CD133 expression. Rapamycin down-regulated HIF-1α expression but up-regulated CD133 expression (Fig. 2*C*). Meanwhile, tacrolimus canceled the effect of rapamycin on the expressions of HIF-1α and CD133 (Fig. 2*D*). These results suggest that the down-regulation of HIF-1α may mediate the up-regulation of CD133 expression in cancer cells. Up-regulation of CD133 expression by rapamycin was reproducibly observed in the CD133 high-expressing cell lines, but not in CD133 low-expressing cell lines (Supplemental Fig. S2).

Induction of HIF-1α down-regulates CD133 expression in cancer cells. Hypoxia mediates the stabilization of HIF-1α protein and enables its escape from rapid degradation, facilitating the up-regulation of HIF-1α expression (12). Hypoxia strongly induced HIF-1α expression, whereas CD133 expression was down-regulated in all three CD133-overexpressing cell lines (Fig. 3*A*). Rapamycin dose-dependently up-regulated CD133 expression under normoxic conditions, but no effect was seen under hypoxic conditions. We speculated that the effect of hypoxia on the induction of HIF-1α is much higher than the effect of rapamycin on the down-regulation of HIF-1α. The expression of CD133 mRNA was also strongly down-regulated under hypoxic conditions in all three cell lines (Fig. 3*B*) and in three additional cell lines (Supplemental Fig. S1).

In addition, DFO, a known HIF-1α activator, induced HIF-1α expression in a dose-dependent manner but down-regulated the expression of CD133 at both the mRNA and protein levels in WiDr cells (Fig. 3*C* and *D*), and in three additional cell lines (Supplemental Fig. S2). These results were consistent with those obtained under hypoxic conditions. Both hypoxia and DFO exposure markedly down-regulated CD133 expression, strongly suggesting that induction of HIF-1α results in the down-regulation of CD133 expression.

Inverse correlation between CD133 and HIF-1α in clinical samples. Finally, to address whether CD133 and HIF-1α expression are inversely correlated in clinical samples of gastric cancer

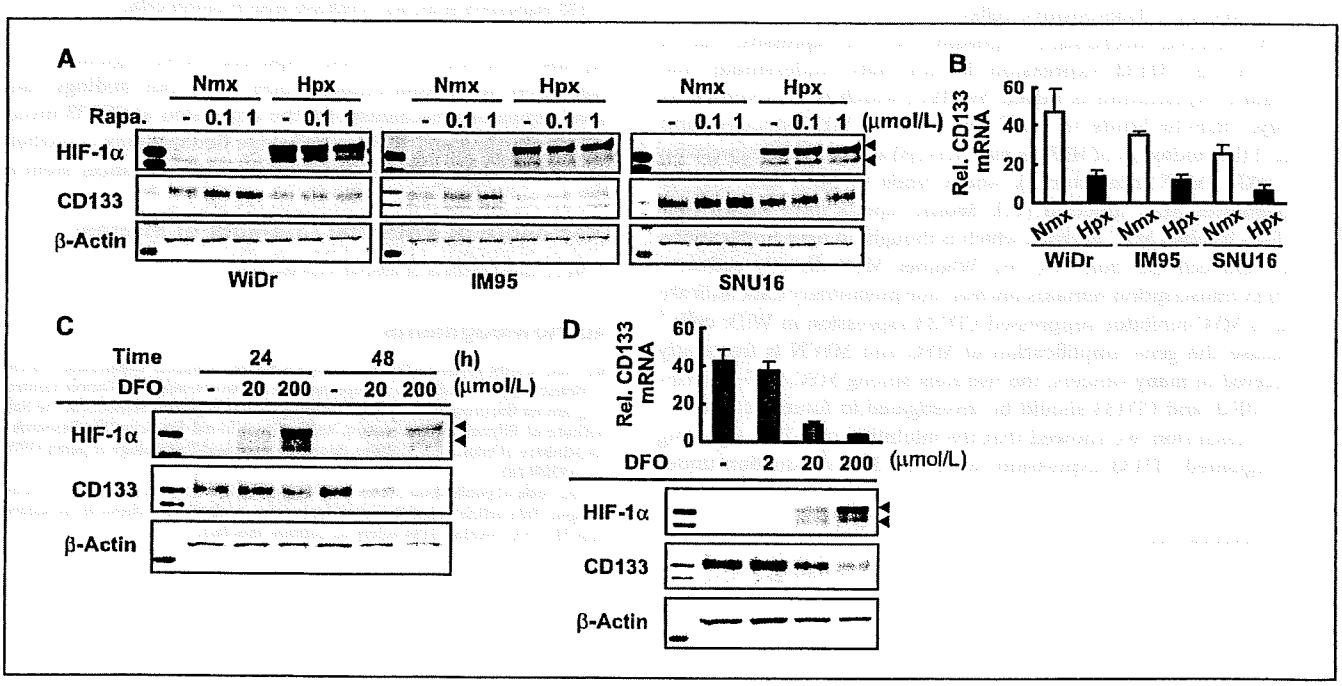

Figure 3. Induction of HIF-1α down-regulates CD133 expression in cancer cells. *A*, three gastrointestinal cancer cell lines were exposed to rapamycin under normoxic or hypoxic conditions for 24 h. Hypoxia induced HIF-1α expression and inversely down-regulated CD133 expression. *B*, hypoxia strongly down-regulated CD133 expression at the mRNA level. *Columns*, mean determined using real-time RT-PCR; *bars*, SD. *C*, DFO, a known HIF-1α activator, induced HIF-1α expression and down-regulated CD133 expression in WiDr cells. *D*, DFO induced these effects at both the mRNA and protein levels. Note that both hypoxia and DFO exposure had similar effects on HIF-1α induction and CD133 down-regulation. *Rel. CD133 mRNA*, normalized mRNA expression levels (CD133/GAPD × 10^4); *Rapa.*, rapamycin.

specimens, we examined the expression of these molecules using previously published microarray data (9). The expressions of CD133 and HIF-1α were inversely correlated in gastric cancer ($r = -0.68$; Fig. 4*A*), whereas the expressions of CD133 and HIF-1β were not ($r = -0.05$; Fig. 4*A*). These results are consistent with the *in vitro* findings in the present study.

Taken together, the present results suggest that an oxygen-sensitive intracellular pathway involving both HIF-1α and mTOR signaling may, at least in part, regulate CD133 expression in cancer cells (shown in the schema in Fig. 4*B*).

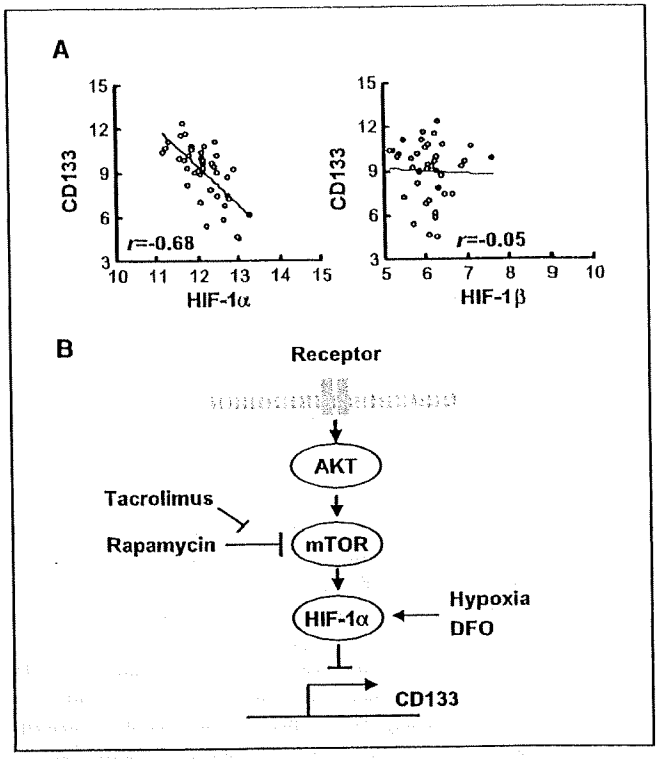

Figure 4. Inverse correlation between CD133 and HIF-1α in clinical samples of gastric cancer. *A*, the correlation between the expressions of CD133 and HIF-1α were analyzed in 40 clinical gastric cancer specimens using previously published microarray data. CD133 and HIF-1α were inversely correlated in gastric cancer ($r = -0.68$), whereas CD133 and HIF-1β were not ($r = -0.05$). *B*, proposed model depicting the involvement of mTOR signaling, HIF-1α, and CD133 expression. HIF-1α, a downstream molecule of mTOR, down-regulates CD133 expression at the transcriptional level in cancer cells.

Discussion

Hypoxic conditions promote the proliferation of mammalian ES cells more efficiently than normoxia and are thought to be required for the maintenance of full pluripotency. Hematopoietic stem cells are located in the bone marrow, which is a physiologically hypoxic environment, and the survival and/or self-renewal of hematopoietic stem cells is enhanced *in vitro* if the cells are cultured under hypoxic conditions (13). Thus, accumulating data indicates that oxygen levels influence specific cell fates in several developmental processes; however, the effect of oxygen levels on cell differentiation is thought to be context-dependent (14). Our data on CD133 expression in response to hypoxia were different from the previous study shown in glioma (5). The discrepancy might be explained by (*a*) a different cellular context in glioma from the others, because CD133 expressions of all cell lines including the WiDr, IM95, SNU16, OCUM1, 44As3, and DLD-1 cells were reproducibly down-regulated by hypoxic condition (Supplemental Fig. S1; Fig. 3*B*), whereas the U251 cells failed to exhibit the down-regulation, and by (*b*) the different detection methods in our study (Western blot and quantitative real-time RT-PCR) from the previous report (flow cytometry for CD133-positive cells).

The detailed mechanism responsible for the repressive role of HIF-1α on CD133 expression is not fully understood; one possible explanation is raised by MYC, which is also known as c-Myc. HIF-1α binds to MAX and renders MYC inactive, and HIF-1 (homodimers of HIF-1α and HIF-1β) activates the expression of MXI1 (MAX interactor 1), which binds to MAX and thereby antagonizes MYC function (11). Recent reports have shown that HIF-1α inhibits MYC activity, which is thought to have implications for stem cell function (15, 16). Whether MYC directly activates CD133 transcription remains unclear; our preliminary data indicate that a MYC-inhibitor suppressed CD133 expression in WiDr cells.[4] Because the gene amplification of MYC and MYCN is frequently observed in many cancers, the relations among MYC, HIF-1α, HIF-1β, HIF-2, and CD133 should be investigated in future studies.

In conclusion, we showed that the inhibition of mTOR signaling up-regulated CD133 expression, whereas HIF-1α induction under hypoxic conditions or DFO exposure down-regulated CD133 expression in gastrointestinal cancer cells. Our findings show a novel regulatory mechanism for the expression of CD133 involving mTOR signaling and HIF-1α, and these findings may contribute to our understanding of the stemness character of cancer stem cells.

[4] Unpublished data.

Disclosure of Potential Conflicts of Interest

No potential conflicts of interest were disclosed.

Acknowledgments

Received 4/7/09; revised 6/2/09; accepted 6/30/09; published OnlineFirst 9/8/09.

Grant support: 3rd Term Comprehensive 10-Year Strategy for Cancer Control, the program for the promotion of Fundamental Studies in Health Sciences of the National Institute of Biomedical Innovation, and a Grant-in-aid for Scientific Research from the Ministry of Education, Culture, Sports, Science and Technology of Japan (19790240 and 19209018).

The costs of publication of this article were defrayed in part by the payment of page charges. This article must therefore be hereby marked *advertisement* in accordance with 18 U.S.C. Section 1734 solely to indicate this fact.

References

1. Neuzil J, Stantic M, Zobalova R, et al. Tumour-initiating cells vs. cancer "stem" cells and CD133: what's in the name? Biochem Biophys Res Commun 2007;355:855–9.
2. Fan X, Matsui W, Khaki L, et al. Notch pathway inhibition depletes stem-like cells and blocks engraftment in embryonal brain tumors. Cancer Res 2006;66:7445–52.
3. Clement V, Sanchez P, de Tribolet N, Radovanovic I, Ruiz i Altaba A. HEDGEHOG-GLI1 signaling regulates human glioma growth, cancer stem cell self-renewal, and tumorigenicity. Curr Biol 2007;17:165–72.
4. Piccirillo SG, Reynolds BA, Zanetti N, et al. Bone morphogenetic proteins inhibit the tumorigenic potential of human brain tumour-initiating cells. Nature 2006;444:761–5.

5. Platet N, Liu SY, Atifi ME, et al. Influence of oxygen tension on CD133 phenotype in human glioma cell cultures. Cancer Lett 2007;258:286–90.
6. Chen HL, Pistollato F, Hoeppner DJ, Ni HT, McKay RD, Panchision DM. Oxygen tension regulates survival and fate of mouse central nervous system precursors at multiple levels. Stem Cells 2007;25:2291–301.
7. Hudson CC, Liu M, Chiang GG, et al. Regulation of hypoxia-inducible factor 1α expression and function by the mammalian target of rapamycin. Mol Cell Biol 2002; 22:7004–14.
8. Chiang GG, Abraham RT. Targeting the mTOR signaling network in cancer. Trends Mol Med 2007;13: 433–42.
9. Yamada Y, Arao T, Gotoda T, et al. Identification of prognostic biomarkers in gastric cancer using endoscopic biopsy samples. Cancer Sci 2008;99: 2193–9.
10. Takeda M, Arao T, Yokote H, et al. AZD2171 shows potent antitumor activity against gastric cancer over expressing FGFR2/KGFR. Clin Cancer Res 2007;13: 3051–7.
11. Dang CV, Kim JW, Gao P, Yustein J. The interplay between MYC and HIF in cancer. Nat Rev Cancer 2008;8: 51–6.
12. Wouters BG, Koritzinsky M. Hypoxia signalling through mTOR and the unfolded protein response in cancer. Nat Rev Cancer 2008;8:851–64.
13. Danet GH, Pan Y, Luongo JL, Bonnet DA, Simon MC. Expansion of human SCID repopulating cells under hypoxic conditions. J Clin Invest 2003;112:126–35.
14. Simon MC, Keith B. The role of oxygen availability in embryonic development and stem cell function. Nat Rev Mol Cell Biol 2008;9:285–96.
15. Koshiji M, Kageyama Y, Pete EA, Horikawa I, Barrett JC, Huang LE. HIF-1α induces cell cycle arrest by functionally counteracting Myc. EMBO J 2004;23: 1949–56.
16. Zhang H, Gao P, Fukuda R, et al. HIF-1 inhibits mitochondrial biogenesis and cellular respiration in VHL-deficient renal cell carcinoma by repression of C-MYC activity. Cancer Cell 2007;11:407–20.

ANTICANCER RESEARCH 29: 1111-1118 (2009)

EGFR Mutation Up-regulates EGR1 Expression through the ERK Pathway

MARI MAEGAWA[1,2], TOKUZO ARAO[1], HIDEYUKI YOKOTE[1], KAZUKO MATSUMOTO[1], KANAE KUDO[1], KAORU TANAKA[1], HIROYASU KANEDA[1], YOSHIHIKO FUJITA[1], FUMIAKI ITO[2] and KAZUTO NISHIO[1]

[1]*Department of Genome Biology, Kinki University School of Medicine, Osaka;*
[2]*Department of Biochemistry, Setsunan University, Osaka, Japan*

Abstract. *Background: DelE746_A750-type EGFR is a constitutively active type of mutation that enhances EGFR signaling. However, the changes in gene expression that occur in mutant EGFR-harboring cells has not been fully studied. Materials and Methods: A gene expression analysis of HEK293 cells transfected with wild-type or mutant EGFR was performed focusing on the significant gene. Results: Early growth response 1 (EGR1), a transcription factor, was the most strongly up-regulated gene in mutant EGFR-transfected cells among the genes examined. An increase in EGR1 expression in the mutant EGFR cells was confirmed using RT-PCR or immunoblotting. The expression was up-regulated by EGF stimulation and down-regulated by EGFR-tyrosine kinase inhibitor. In addition, the MEK inhibitor U0126 inhibited EGR1 expression, while the phosphatidylinositol 3-kinase inhibitor LY294002 did not. Conclusion: Mutant EGFR constitutively up-regulates EGR1 through the ERK pathway, and its expression is correlated with EGFR signal activation. Findings provide an insight into a target gene of mutant EGFR and further improve the understanding of the oncogenic properties of EGFR.*

Epidermal growth factor receptor (EGFR) is frequently overexpressed in various solid tumors (1, 2) and is regarded as a definitive oncogene. Accumulating data on EGFR and its signal pathway in cancer cells suggests that EGFR is a promising therapeutic target molecule; indeed, benefits from treatment with EGFR tyrosine kinase inhibitors (EGFR-TKIs) and anti-EGFR antibody have been confirmed in clinical settings (3, 4). Common *EGFR* mutations of DelE746_A750 and L858R, characterized by 15-base in-frame deletions or substitutions clustered around the ATP-binding site in exons 19 and 21 of *EGFR*, have been identified in patients with non-small cell lung cancer (NSCLC); these mutations are major determinants of sensitivity to EGFR-TKIs (5-8). Such mutations confer a constitutively active EGFR signal pathway to cancer cells (9).

The activated EGFR signal pathway has been intensively investigated, including studies on alterations in downstream signaling, the underlying mechanism responsible for sensitivity to EGFR-TKIs, the involvement in carcinogenesis, oncogene addiction, and clinico-pathological analyses. It has been previously reported that a lung cancer cell line, PC-9, with a deletional mutant of *EGFR* (delE746_A750) was hypersensitive to EGFR-TKIs and that this mutant *EGFR* was constitutively active and activated the ERK and AKT pathways (10-13). However, the changes in gene expression that occur in mutant *EGFR*-harboring cells have not been fully studied.

To identify changes in the gene expressions of downstream molecules that arise as a result of *EGFR* mutation and activated EGFR signaling, a microarray analysis of cells, in which the DelE746_A750-type of *EGFR* mutation had been stably introduced, was performed.

Materials and Methods

Reagents. The purified recombinant human EGF was purchased from R&D systems (Minneapolis, MN, USA). LY294002 2-(4-Morpholinyl)-8-phenyl-4H-benzopyran- 4-one was purchased from Calbiochem (San Diego, CA, USA), U0126 1,4-diamino-2,3-dicyano-1,4-bis[2-aminophenylthio] butadine was purchased from Cell Signaling Technology (Beverly, MA, USA).

Expression constructs and viral production. Full-length cDNA of wild-type *EGFR* was amplified by RT-PCR from a human embryonal kidney cell line (HEK293), and mutant *EGFR* (delE746_A750) was amplified from an NSCLC cell line (PC-9) (10, 14). Wild-type and mutant *EGFR* cDNA in a pcDNA3.1 vector (Clontech, Palo Alt, CA, USA) was cut out and introduced into a pQCLIN retroviral vector (BD Biosciences Clontech, San Diego, CA, USA) together with EGFP, followed by the internal ribosome entry sequence (IRES) to monitor the expression of the inserts indirectly. A pVSV-G vector (Clontech,

Correspondence to: Kazuto Nishio, Department of Genome Biology, Kinki University School of Medicine, 377-2 Ohno-higashi, Osaka-Sayama, Osaka 589-8511, Japan. Tel: +81 723676369, Fax: +81 723660206, e-mail: knishio@med.kindai.ac.jp

Key Words: EGFR, EGR1, microarray, mutation.

0250-7005/2009 $2.00+.40

Palo Alt, CA, USA) for the constitution of the viral envelope and pQCXIX constructs were co-transfected into the GP2-293 cells using FuGENE6 transfection reagent. Briefly, 80% confluent cells cultured on a 10-cm dish were transfected with 2 μg of pVSV-G plus 6 μg of pQCXIX vectors. Forty-eight hours after transfection, the culture medium was collected and the viral particles were concentrated by centrifugation at 15,000 g for 3 h at 4°C. The viral pellet was then resuspended in fresh RPMI1640 medium. The titer of the viral vector was calculated by counting the EGFP-positive cells that were infected by serial dilutions of virus-containing medium, and the multiplicity of infection (MOI) was then determined.

Cell culture and transfection. The HEK293 cell line was cultured in DMEM (Sigma, St. Louis, MO, USA) supplemented with 10% fetal bovine serum (FBS), penicillin and streptomycin (Sigma) in a humidified atmosphere of 5% CO_2 at 37°C. The HEK293 cells were retrovirally transfected with the mock, wild-type and mutant *EGFR*, and the stable established cell lines were designated as HEK293-Mock, HEK293-Wild and HEK293-Del.

Real-time RT-PCR. One microgram of total RNA from a cultured cell line was converted to cDNA using a GeneAmp® RNA-PCR kit (Applied Biosystems, Foster City, CA, USA). Real-time PCR was carried out using the Applied Biosystems 7900HT Fast Real-time PCR System (Applied Biosystems) under the following conditions: 95°C for 6 min, and 40 cycles of 95°C for 15 sec and 60°C for 1 min. *GAPD* was used to normalize the expression levels in the subsequent quantitative analyses. To amplify the target genes, the following primers were purchased from TaKaRa (Yotsukaichi, Japan): EGR1-FW, GTA CAG TGT CTG TGC CAT GGA TTT C; EGR1-RW, GAG GAT CAC CAT TGG TTT GCT TG; GAPD-FW, GCA CCG TCA AGG CTG AGA AC; and GAPD-RW, ATG GTG GTG AAG ACG CCA GT. The results of three independent experiments were analyzed.

In vitro growth-inhibition assay. The growth-inhibitory effects of AG1478 (Biomol International, Plymouth Meeting, PA, USA) on the HEK293-Mock, -Wild and -Del cells were examined using an MTT assay. A 180-μL volume of an exponentially growing cell suspension (2×10^3 cells/well) was seeded into 96-well microtiter plates and 20 μL of various drug concentrations were added. After incubation for 72 h at 37°C, 20 μL of MTT solution (5 mg/mL in PBS) were added to each well and the plates were incubated for an additional 3 h at 37°C. After centrifuging the plates at 400 g for 5 min, the medium was aspirated from each well and 200 μL of DMSO was added to each well to dissolve the formazan. The optical density was measured at 570 nm. The results of three independent experiments were analyzed.

Immunoblotting. The antibodies used for immunoblotting were as follows: anti-EGFR (Upstate Biotechnology), anti-phospho-EGFR (Tyr1068), anti-p44/42 MAP kinase, anti-phospho-p44/42 MAP kinase, anti-Akt (Cell Signaling), anti-EGR1, anti-βactin (Santa Cruz), and anti-phospho-Akt (Ser473) (BD Bioscience, SanJose, CA, USA). Sub-confluent cells were washed with cold PBS and harvested with Lysis A buffer containing 1% Triton X-100, 20 mM Tris-HCl (pH 7.0), 5 mM EDTA, 50 mM sodium chloride, 10 mM sodium pyrophosphate, 50 mM sodium fluoride, 1 mM sodium orthovanadate, and a protease inhibitor mix, complete™ (Roche Diagnostics). Whole-cell lysates and the culture medium were separated using a 2-15% gradient SDS-PAGE and blotted onto a polyvinylidene fluoride membrane. After blocking with 3% bovine serum albumin in a TBS buffer (pH 8.0) with 0.1% Tween 20, the membrane was probed with primary antibody. After rinsing twice with TBS buffer, the membrane was incubated with horseradish peroxidase (HRP)-conjugated secondary antibody (Cell Signaling) and washed, followed by visualization using an ECL detection system (Amersham) and LAS-3000 (Fujifilm, Tokyo, Japan). The immunoblotting was performed in two independent experiments.

Microarray analysis. The microarray procedure was performed according to the Affymetrix protocols (Santa Clara, CA, USA). In brief, the total RNA extracted from the cell lines was analyzed using an Agilent 2100 Bioanalyzer (Agilent Technologies, Waldbronn, Germany) as a quality check, and cRNA was synthesized using the GeneChip® 3'-Amplification Reagents One-Cycle cDNA Synthesis Kit (Affymetrix). The labeled cRNAs were then purified and used to construct the probes. Hybridization was performed using the Affymetrix GeneChip HG-U133 Plus2.0 array for 16 h at 45°C. The signal intensities were measured using a GeneChip®Scanner3000 (Affymetrix) and converted to numerical data using the GeneChip Operating Software, Ver.1 (Affymetrix).

Statistical analysis. The microarray analysis was performed using the BRB Array Tools software ver. 3.3.0 (http://linus.nci.nih.gov/BRB-ArrayTools.html), developed by Dr. Richard Simon and Dr. Amy Peng. The microarray analysis was performed as described previously (15). Additional statistical analyses were performed using Microsoft Excel (Microsoft, Redmond, WA, USA) to calculate the standard deviation (SD) and statistically significant differences between each sample using the Student *t*-test. *P*-values of <0.05 were considered statistically significant.

Results

Early growth response 1 (EGR1) expression in mutant EGFR. The DelE746_A750-type *EGFR* mutation mediates a constitutively active EGFR signal and induces cellular hypersensitivity to EGFR-TKIs (11, 13). Mock, wild and mutant *EGFR* was introduced and stable cell lines was established as HEK293-Mock, -Wild and -Del cells. HEK293-Del cells showed increased phosphorylation levels of EGFR and ERK1/2 and were significantly hypersensitive to the EGFR-tyrosine kinase inhibitor AG1478, compared with the other cell lines (Figure 1A and 1B). To identify which gene expressions were changed by the *EGFR* mutation, a microarray analysis was performed for these stable cell lines. Twenty-three genes were identified as differentially expressed genes, the expressions of which differed by more than three-fold between HEK293-Wild and HEK293-Del cells (Table I). These genes included several cancer-related genes such as *EGR1, GALNT3, TACSTD1* (EpCAM), *MAFF, NLK, FOXN4, RUNX3* and *CD70*. Among them, *EGR1* was the most up-regulated gene in the HEK293-Del cells (>10-fold higher than in HEK293-Mock and -Wild cells, Figure 1C, 1D). The ratios of the signal intensity relative to that in the HEK293-Mock cells were 3.0-fold in the HEK293-Wild cells and 34.5-fold in the HEK293-Del

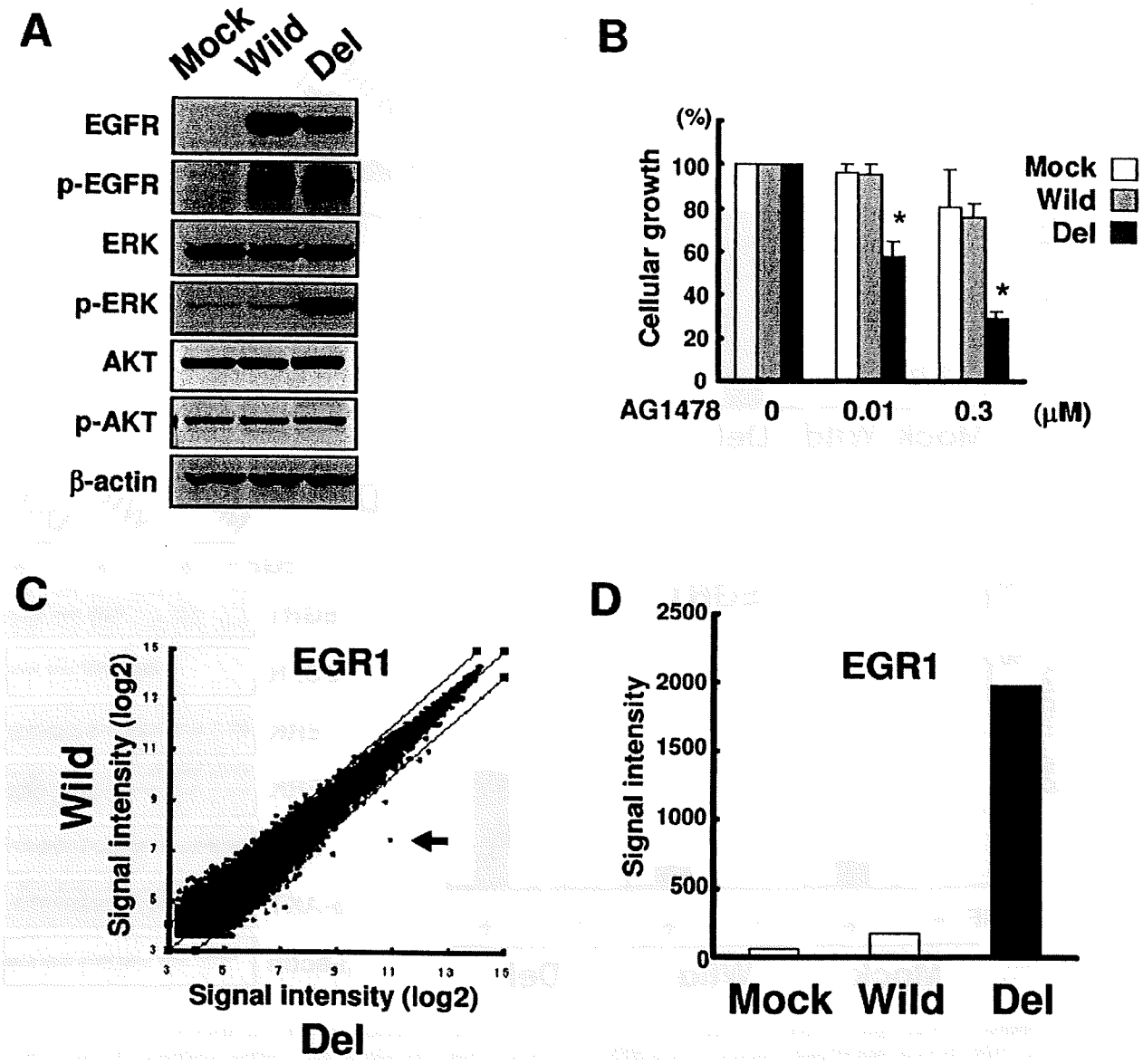

Figure 1. *Microarray analysis showing that mutant EGFR up-regulates EGR1 expression. (A) Immunoblotting for HEK293-Mock, -Wild and -Del cells cultured under normal conditions. The phosphorylation of EGFR and ERK1/2 was increased in HEK293-Del cells. (B) Growth inhibitory effect of an EGFR tyrosine kinase inhibitor. HEK293-Del cells were highly sensitive to AG1478. (C) Results of microarray analysis for genes with differential expressions between HEK293-Wild and -Del cells. The arrow indicates the EGR1 gene. (D) Signal intensity of microarray data for EGR1. EGR1 expression was up-regulated by more than 10-fold, compared with in HEK293-Wild cells. The error bars represent the SDs of three independent experiments. *: $p<0.05$.*

cells. Thus, the role of the *EGR1* transcription factor in EGFR signal activation was the focus of subsequent studies.

EGF stimulates EGR1 expression. The mRNA and protein levels of EGR1 up-regulation were confirmed using real-time RT-PCR and western blotting for these stable cell lines. Real-time RT-PCR revealed that *EGR1* mRNA expression in the HEK293-Wild cells was slightly (~3-fold) higher than that in the HEK293-Mock cells. On the other hand, *EGR1* mRNA expression was remarkably increased in the HEK293-Del cells (133-fold, compared with the HEK293-Mock cells). Similar results were obtained for the protein levels (Figure 2A, 2B). These results indicate that *EGR1* expression was constitutively up-regulated in the *EGFR* mutation-harboring cells.

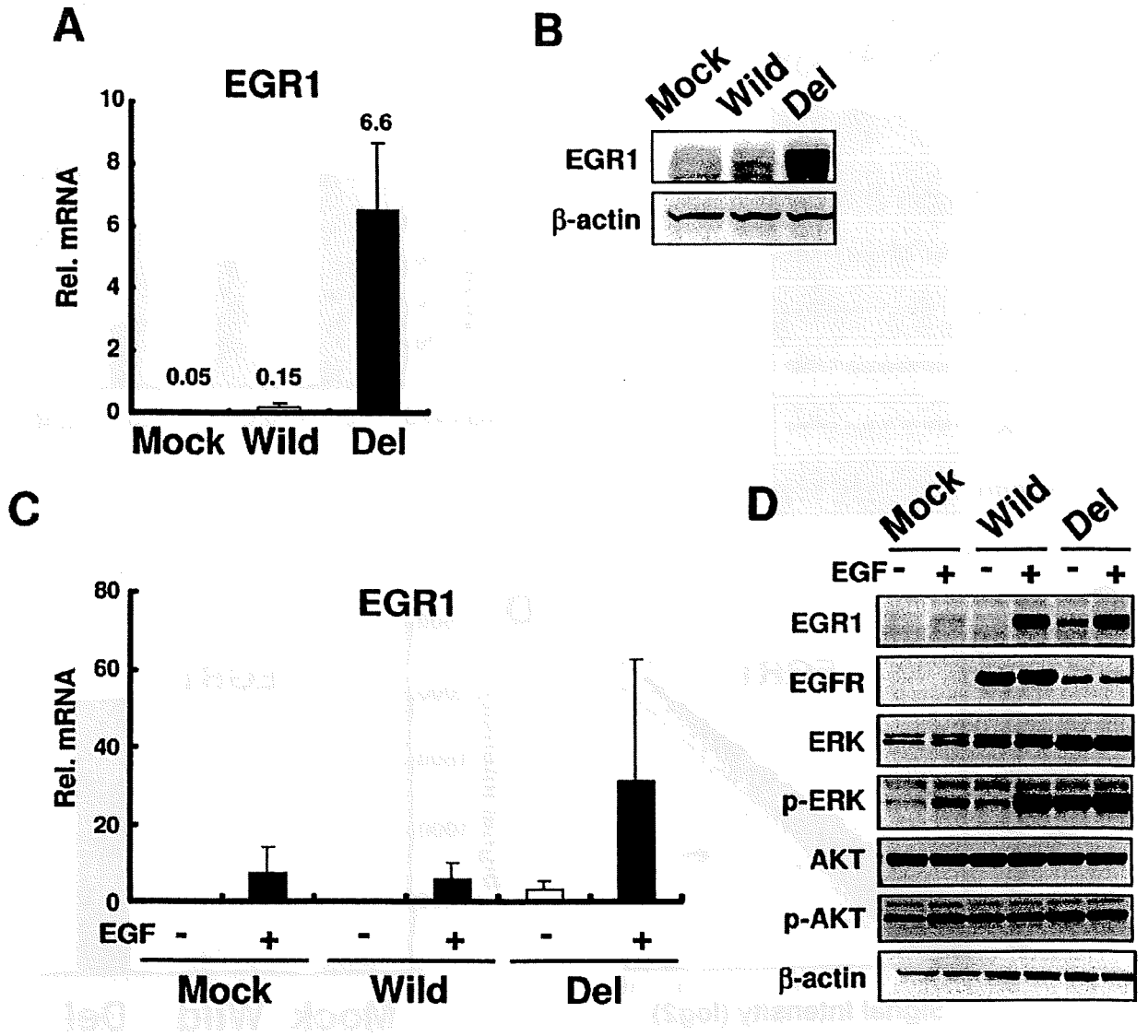

Figure 2. *Mutant EGFR up-regulates EGR1, and EGR1 expression is regulated by EGF stimulation. (A) Real-time RT-PCR shows that mutant EGFR up-regulates EGR1 by more than 40-fold, compared with in HEK293-Mock and -Wild cells cultured under normal conditions. (B) Immunoblotting shows the up-regulation of EGR1 in HEK293-Del cells. (C, D) EGF stimulation and EGR1 expression detected by real-time RT-PCR and immunoblotting. EGR1 expression was up-regulated by EGF, and the expression was correlated with the phospho-ERK1/2 levels. The error bars represent the SDs of three independent experiments. Immunoblotting was performed in two independent experiments. Rel. mRNA indicates the ratio of mRNA expression of EGR1/GAPD* $\times 10^{-6}$.

To examine whether the up-regulation of *EGR1* expression is regulated by EGFR signaling, the change in expression induced by EGF stimulation was evaluated. EGF increased *EGR1* mRNA expression in HEK293-Mock, -Wild and -Del cells (Figure. 2C). EGR1 up-regulation by EGF was also confirmed by immunoblotting (Figure 2D). HEK293-Wild cells stimulated with EGF expressed EGR1 to the same extent as in HEK293-Del cells, possibly reflecting the constitutively active function of EGFR in the HEK293-Del cells. In addition, EGR1 expression was closely correlated with the phospho-ERK1/2 expression levels. These findings suggest that EGR1 expression is involved in the ERK1/2 pathway.

EGFR-TKI down-regulates EGR1 expression. To elucidate the further relationship between *EGR1* up-regulation and EGFR signaling activity, the three cell lines were treated with EGFR-TKI. An EGFR-TKI, AG1478, inhibited the

Table I. *The results of microarray analysis for differentially expressed genes between HEK293 Wild and HEK293 Del cells. Twenty-three genes were identified as differentially expressed genes, the expressions of which differed by more than three fold.*

Gene	Description	Probe set	Wild	Del	Fold change
EGR1	Early growth response 1	227404_s_at	172	1979	11.5
APOBEC3B	Apolipoprotein B mRNA editing enzyme	206632_s_at	27	147	5.4
GALNT3	UDP-N-acetyl-alpha-D-galactosamine	203397_s_at	118	477	4.1
TACSTD1	Tumor-associated calcium signal transducer 1	201839_s_at	23	91	3.9
MAFF	Transcription factor MAFF	36711_at	29	114	3.9
LOC646903	Hypothetical LOC646903	237116_at	19	67	3.6
UCHL1	Ubiquitin carboxyl-terminal esterase L1	201387_s_at	483	1733	3.6
RABL3	RAB, member of RAS oncogene family-like 3	226090_x_at	12	39	3.2
ZNF330	Zinc finger protein 330	213760_s_at	47	149	3.2
ERGIC2	ERGIC and golgi 2	226422_at	66	208	3.2
PHLDA2	Pleckstrin homology-like domain, family A, member 2	209803_s_at	59	183	3.1
TRIM5	Tripartite motif-containing 5	210705_s_at	13	40	3.1
KLHL23	Kelch-like 23 (Drosophila)	213610_s_at	62	192	3.1
C18orf37	Chromosome 18 open reading frame 37	1559716_at	56	13	0.23
NLK	Nemo-like kinase	238624_at	59	15	0.25
	CDNA FLJ34034 fis	238515_at	41	11	0.27
FOXN4	Forkhead box N4	241009_at	57	15	0.27
RUNX3	Runt-related transcription factor 3	204198_s_at	44	13	0.28
	transcribed locus	230746_s_at	70	21	0.31
CD70	CD70 molecule	206508_at	80	25	0.31
VDAC1	Voltage-dependent anion channel 1	217139_at	52	16	0.31
NBEA	Neurobeachin	226439_s_at	33	10	0.32
NID2	Nidogen 2 (osteonidogen)	204114_at	55	18	0.32

expression of both *EGR1* mRNA (Figure 3A) and protein (Figure 3B). EGR1 expression was also correlated with the phospho-ERK1/2 expression levels detected by immunoblotting. These results support the concept that EGR1 up-regulation by mutant EGFR is regulated by EGFR signaling.

EGR1 expression is regulated through the ERK1/2 pathway. EGR1 is thought to be a downstream molecule in the ERK1/2 pathway (16). To elucidate whether EGR1 up-regulation in mutant EGFR cells is regulated *via* the ERK1/2 pathway, ERK1/2 and AKT, two major downstream pathways of EGFR was evaluated. LY294002, a phosphatidylinositol 3-kinase inhibitor, inhibited the phosphorylation levels of AKT but did not modify the expression of EGR1 (Figure 4A). However, the MEK inhibitor U0126 clearly down-regulated EGR1 expression in HEK293-Del cells (Figure 4B). EGR1 expression was consistent with the phospho-ERK1/2 expression levels. These results strongly suggest that EGR1 up-regulation by mutant *EGFR* is regulated through the ERK pathway. Based on these findings, a model was propossed to explain the up-regulation of EGR1 by mutant *EGFR* (Figure 4C). In this model, mutant *EGFR* activates the ERK pathway and induces *EGR1* transcription.

Discussion

EGR1 transcription factor is induced by various stimuli, including growth factors, hypoxia, UV and cytokines, and mediates multiple cellular responses such as mitogenesis, differentiation, cellular survival, anti-apoptosis, angiogenesis and apoptosis (17). In cancer biology, *EGR1* is basically regarded as a tumor suppressor gene because it directly regulates p53, PTEN and TGFβ1. Deletion of the *EGR1*-containing 5q31 region has been associated with a certain type of lymphoma and small cell lung carcinoma. Low EGR1 expression in tumor tissue is frequently observed in breast cancer, glioblastoma and other solid tumors (18). In contrast, the oncogenic property of *EGR1* is observed in prostate cancer (19).

An increased expression of *EGR1* was observed in mutant *EGFR* cells. Previous reports have demonstrated that mutant *EGFR* is oncogenic in non-small cell lung cancer (20). However, Ferraro *et al.* have demonstrated that *EGR1* expression is strongly correlated with PTEN expression and that patients with high levels of EGR1 had better overall and disease-free survival periods than patients with low levels of EGR1 in patients with NSCLC (21). It was speculated that the overexpression of EGR1 in mutant *EGFR* cells may play some role in the biological behaviors of mutant *EGFR* in cancer.

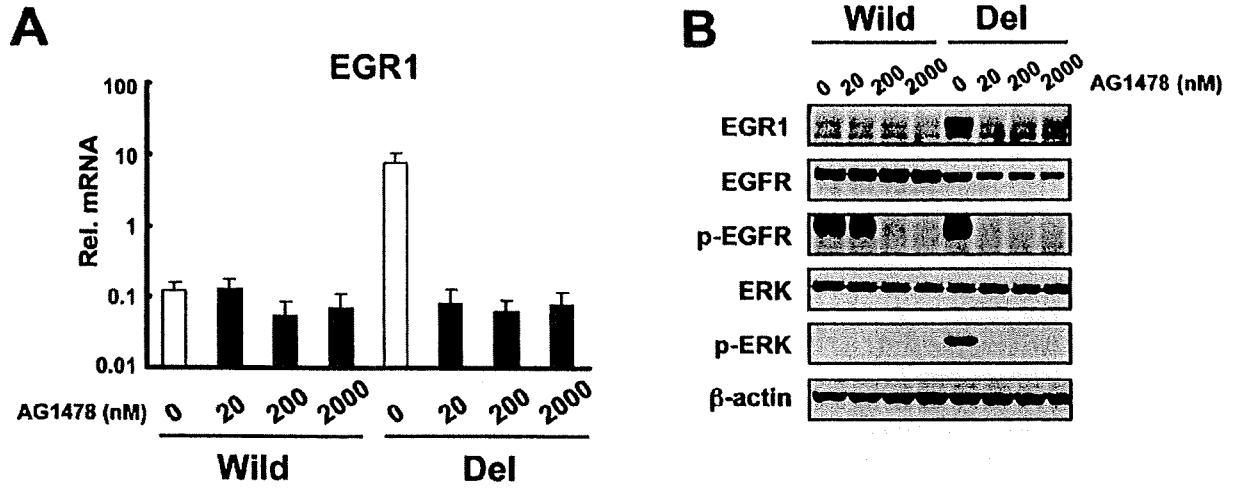

Figure 3. *EGFR tyrosine kinase inhibitor down-regulates EGR1 expression. (A) Real-time RT-PCR and (B) immunoblotting were performed for cells cultured under normal conditions and treated with four concentrations of AG1478 for 5 h. EGFR tyrosine kinase inhibitor clearly down-regulated EGR1 expression. The phosphorylation levels of EGFR decreased at a lower concentration (20 nM) in HEK293-Del cells than in HEK293-Wild cells. Note that the Y-axis is a log-scale. Error bars represent the SDs of three independent experiments. Immunoblotting was performed in two independent experiments. Rel. mRNA indicates the ratio of mRNA expression of EGR1/GAPD × 10 ^{6}.*

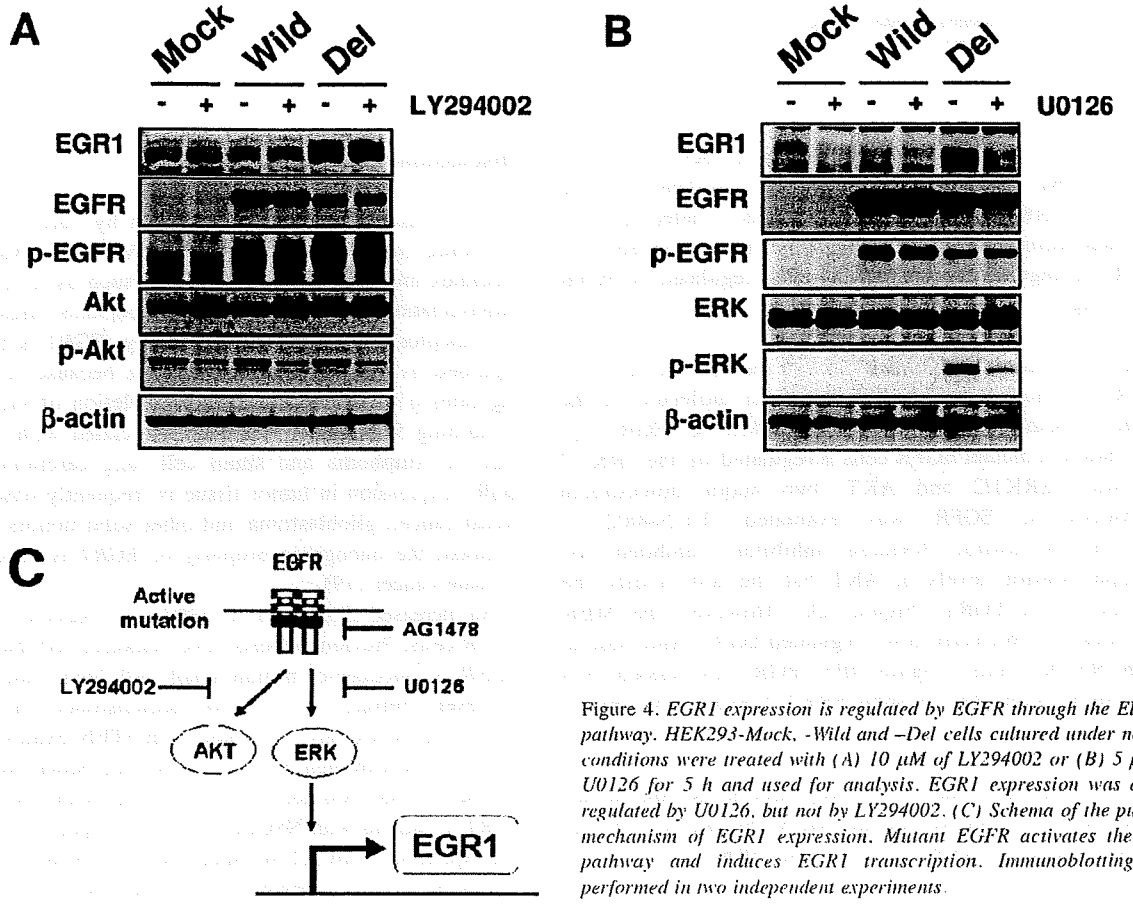

Figure 4. *EGR1 expression is regulated by EGFR through the ERK1/2 pathway. HEK293-Mock, -Wild and -Del cells cultured under normal conditions were treated with (A) 10 μM of LY294002 or (B) 5 μM of U0126 for 5 h and used for analysis. EGR1 expression was down-regulated by U0126, but not by LY294002. (C) Schema of the putative mechanism of EGR1 expression. Mutant EGFR activates the ERK pathway and induces EGR1 transcription. Immunoblotting was performed in two independent experiments.*